Molecular Probes

DOI: 10.1002/anie.201210279

Red Fluorescent Probe for Monitoring the Dynamics of Cytoplasmic Calcium Ions**

*Takahiro Egawa, Kazuhisa Hirabayashi, Yuichiro Koide, Chiaki Kobayashi, Naoya Takahashi, Tomoko Mineno, Takuya Terai, Tasuku Ueno, Toru Komatsu, Yuji Ikegaya, Norio Matsuki, Tetsuo Nagano, and Kenjiro Hanaoka**

The development of sophisticated fluorescent probes has contributed to the elucidation of the molecular mechanisms of many complex biological phenomena.[1–4] In particular, fluorescence imaging of the calcium ion (Ca^{2+}) has become an essential technique for the investigation of signaling pathways involving Ca^{2+} as a second messenger. For example, changes in the intracellular Ca^{2+} concentration have been found to be related to physiological responses in obesity, as well as immune responses and pathological responses in Alzheimer's disease.[5–10] Because Ca^{2+} signaling is involved in so many biological phenomena,[11,12] it is expected that the simultaneous visualization of Ca^{2+} and other biomolecules, that is, multicolor imaging, would be particularly informative. For this purpose, we require a fluorescent probe for Ca^{2+} that operates in a different color window from that of probes for other molecules.

Fluorescent Ca^{2+} sensors can be categorized into two main classes: those based on genetically encoded fluorescent proteins[13,14] and those based on fluorescent small organic molecules.[5] Although both types of sensors have certain advantages and drawbacks, small-molecule-based probes have the particular advantage that their AM ester form (cell-permeable acetoxymethyl ester derivative) can be readily bulk loaded into live cells with no need for transfection. Most currently used small-molecular fluorescent probes for Ca^{2+} are fluorescein-based, such as Fluo-3, Fluo-4, Calcium Green-1, and Oregon Green 488 BAPTA-1, and emit green fluorescence (ca. 527 nm).[15–17] There are also some red-emitting fluorescent probes for Ca^{2+}, such as Rhod-2 (ca. 576 nm), which is based on the rhodamine scaffold.[15] These red-emitting fluorescent probes for Ca^{2+}, including Rhod-2, are also widely used for biological studies; however, the cationic nature of the rhodamine scaffold generally causes Rhod-2 AM to localize into mitochondria.[18] Although this behavior is useful for monitoring the Ca^{2+} dynamics of mitochondria, the visualization of cytoplasmic Ca^{2+} is much more important for research on Ca^{2+} signaling. The influx of Ca^{2+} into the cytoplasm from the extracellular environment and/or from intracellular stores (including the endoplasmic reticulum) triggers numerous cellular responses mediated by the interaction of Ca^{2+} with various Ca^{2+}-binding proteins, such as calmodulin and troponin C.[11,12] Fura Red is a representative near-infrared fluorescent probe for Ca^{2+} that is often used in biological research. However, it has extremely low fluorescence quantum efficiency ($\Phi_{fl} \approx 0.013$).[19] Accordingly, the fluorescence signal is very small unless a high concentration of Fura Red or a high-powered laser is used. However, the use of a high dye concentration has a buffering effect on Ca^{2+}, whereas the use of a high laser power causes rapid photobleaching of the dye and phototoxicity to the cells. Thus, a novel fluorescent probe for cytoplasmic Ca^{2+} with strong emission in the long-wavelength region would be extremely useful, especially for multicolor imaging. In the present study, we designed and synthesized a novel and practical red-fluorescence-emitting probe suitable for monitoring cytoplasmic Ca^{2+} and confirmed its usefulness for the visualization of stimulus-induced Ca^{2+} oscillation in HeLa cells.

As a fluorophore that emits in the red region, we chose TokyoMagenta (TM). The absorption and fluorescence wavelengths of this fluorescein analogue are 90 nm longer than those of fluorescein.[20] TM was also expected to retain the advantages of the fluorescein scaffold, including cytoplasmic localization. For the development of the red fluorescent probe, we chose a combination of 2-Me-substituted TM as the fluorescent moiety and 1,2-bis(*o*-aminophenoxy)ethane-*N*,*N*,*N*′,*N*′-tetraacetic acid (BAPTA) as a specific chelator for Ca^{2+}, and synthesized CaTM-1 (Figure 1; see also Scheme S1 in the Supporting Information).

The fluorescence-activation ratio of CaTM-1 in the presence/absence of Ca^{2+} is 5.6:1 (Figure 2a,b, Table 1). To further improve this ratio, we decided on the strategy of decreasing the energy of the highest occupied molecular orbital (HOMO) of the fluorophore to obtain a high level of

[*] T. Egawa, K. Hirabayashi, Dr. Y. Koide, C. Kobayashi, Dr. N. Takahashi, Dr. T. Terai, Dr. T. Ueno, Dr. T. Komatsu, Dr. Y. Ikegaya, Prof. N. Matsuki, Prof. T. Nagano, Dr. K. Hanaoka
Graduate School of Pharmaceutical Sciences
The University of Tokyo
7-3-1 Hongo, Bunkyo-ku, Tokyo 113-0033 (Japan)
E-mail: khanaoka@mol.f.u-tokyo.ac.jp
Dr. T. Mineno
Faculty of Pharmacy, Takasaki University of Health and Welfare
60 Nakaorui, Takasaki-shi, Gunma 370-0033 (Japan)

[**] This research was supported in part by the Ministry of Education, Culture, Sports, Science and Technology of Japan (Specially Promoted Research Grant No. 22000006 to T.N.), SENTAN, the JST (grant to K.H.), and the Funding Program for Next Generation World-Leading Researchers (LS023 to Y.I.). K.H. was also supported by grants from the Inoue Foundation for Science, the Takeda Science Foundation, the Tokyo Biochemical Research Foundation, and the Astellas Foundation for Research on Metabolic Disorders.

Supporting information for this article is available on the WWW under http://dx.doi.org/10.1002/anie.201210279.

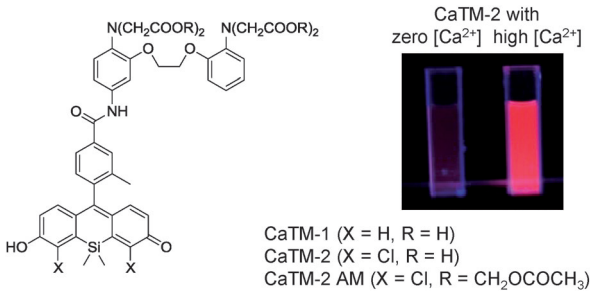

Figure 1. Left: Chemical structures of the red fluorescent Ca^{2+} probes CaTM-1, CaTM-2, and CaTM-2 AM (a cell-permeable derivative of CaTM-2). Right: Photographs of an aqueous solution of CaTM-2 in the absence of Ca^{2+} and in the presence of free Ca^{2+} ions (39 μM) under UV irradiation (365 nm).

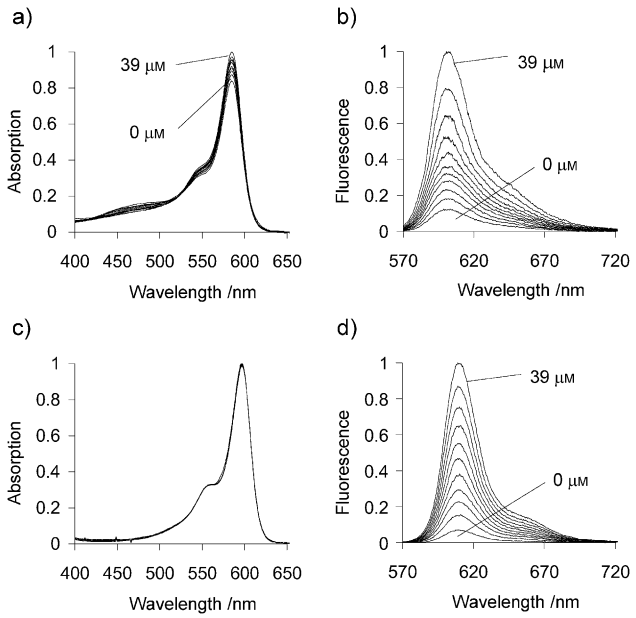

Figure 2. a,b) Ca^{2+}-dependent absorption (a) and emission (b) spectra of CaTM-1 (1 μM) in the presence of free Ca^{2+} ions at various concentrations (0, 0.017, 0.038, 0.065, 0.100, 0.150, 0.225, 0.351, 0.602, 1.35, 39 μM) in 3-(*N*-morpholino)propanesulfonic acid (MOPS) buffer (30 mM) containing KCl (100 mM) and ethyleneglycol tetraacetic acid (EGTA; 10 mM) at pH 7.2 and 22 °C. The excitation wavelength was 550 nm. The relative absorption and relative fluorescence intensity are shown. c,d) Ca^{2+}-dependent absorption (c) and emission (d) spectra of CaTM-2 (1 μM) under the same conditions as in (a,b).

Table 1: Photophysical properties of CaTM-1 and CaTM-2.[a]

	$[Ca^{2+}]=0$ μM			$[Ca^{2+}]=39$ μM			
	λ_{abs} [nm]	λ_{fl} [nm]	Φ_{fl}	λ_{abs} [nm]	λ_{fl} [nm]	Φ_{fl}	K_d [μM]
CaTM-1	585	603	0.066	585	603	0.37	0.38
CaTM-2	597	609	0.024	597	609	0.39	0.20

[a] Measurements were made in a buffer under the conditions described in Figure 2 in the absence and presence of free Ca^{2+} ions.

quenching by photoinduced electron transfer in the absence of Ca^{2+}.[21] With this aim, we introduced chlorine into the fluorophore to produce dichloro-TokyoMagenta (DCTM; see Figure S1 in the Supporting Information). The HOMO energy level of DCTM was calculated to be lower than that of TM (see Table S1 in the Supporting Information). We then developed a novel Ca^{2+} probe, CaTM-2, based on DCTM (Figure 1; see also Scheme S1 in the Supporting Information). As we had hoped, the activation ratio of CaTM-2 was considerably improved (16:1) with respect to that of CaTM-1, presumably owing to stabilization of the HOMO energy level of the fluorophore moiety (Figure 2c,d, Table 1).

The chlorination of the fluorophore was also advantageous in another respect. As we have previously reported, TM shows pH dependency: the absorption wavelength is markedly blue-shifted under acidic conditions (see Figures S2–S4 and Table S2 in the Supporting Information),[20] and CaTM-1 showed similar behavior (Figure 3). This property can

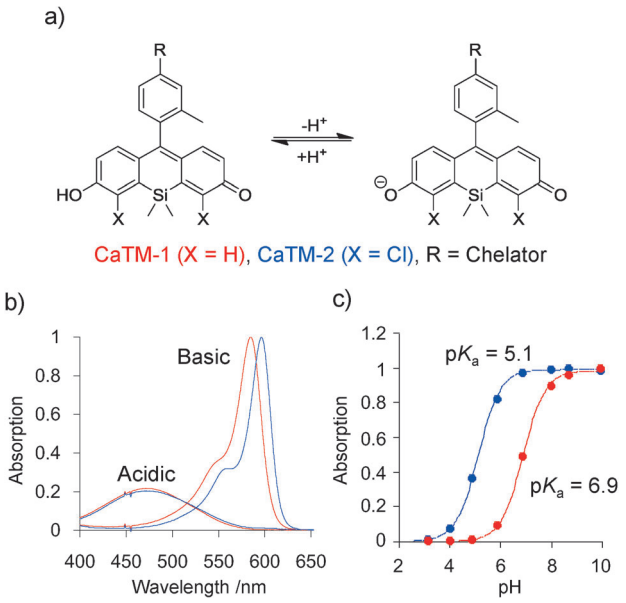

Figure 3. pH dependency of CaTM-1 and CaTM-2. a) pH-dependent equilibrium of CaTM-1 and CaTM-2 in an aqueous buffer. b) Absorption spectra of CaTM-1 (red) and CaTM-2 (blue) in acidic (pH 3) and basic (pH 9) sodium phosphate buffer containing ethylenediaminetetraacetic acid (EDTA; 5 mM). For convenience for comparison, the relative absorption is shown, that is, the maximum absorption of each anion form was defined as 1.0. c) Curve fittings of pH-dependent changes in the normalized absorbance of CaTM-1 (red) and CaTM-2 (blue) at the absorption maximum for each anion form (right-hand structure in Figure 3a; 585 nm for CaTM-1 and 597 nm for CaTM-2) in sodium phosphate buffer containing EDTA (5 mM).

reduce the fluorescence signal under physiological conditions (pH 7.4), and a sufficiently low pK_a value of the probe is required for biological applications. Fortunately, the pK_a value of CaTM-2 was greatly shifted into the acidic region relative to that of CaTM-1 (Figure 3), and was sufficiently low ($pK_a=5.1$) for practical use. This pK_a value is derived from that of the fluorophore itself (Figure 3a), that is, the lower pK_a value of CaTM-2 is due to the electron-withdrawing character of chlorine (see Figures S2–S5 and Table S2 in the Supporting Information). We next examined the suitability of CaTM-2 as a red fluorescent probe for monitoring cytoplasmic Ca^{2+} in cells.

For cellular applications, we synthesized CaTM-2 AM, an AM ester form of CaTM-2 (Figure 1; see also Scheme S1 in the Supporting Information). Because of the hydrophilicity of the BAPTA moiety, Ca^{2+} indicators, including CaTM-2, generally cannot pass through cell membranes without the use of special procedures, such as electroporation.[22] In contrast, AM ester forms of Ca^{2+} probes can readily enter cells, where they are enzymatically cleaved by intracellular esterase to afford the Ca^{2+}-sensitive, cell-impermeable form.

To examine the potential of CaTM-2 for multicolor imaging, we loaded HeLa cells expressing cyan fluorescent protein (CFP; localized to the nucleus) and yellow fluorescent protein (YFP; localized to the Golgi apparatus) with CaTM-2 AM (Figure 4). The fluorescence of CaTM-2 in the red region was clearly separable from the signals of CFP and YFP. Thus, the multicolor imaging of cytoplasmic Ca^{2+} simultaneously with plural biomolecules can be carried out by utilizing CaTM-2 AM together with fluorophores whose fluorescence wavelengths are in the yellow or shorter-wavelength region (including well-established fluorescent protein-based sensors).[13,23]

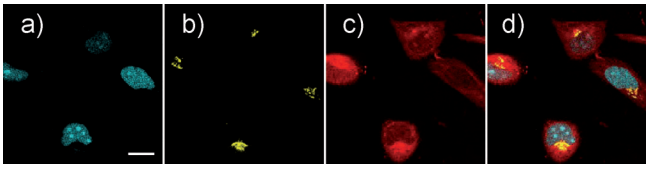

Figure 4. Triple-color imaging of CFP, YFP, and CaTM-2 in HeLa cells. a–c) CFP–nucleus (a, cyan channel) and YFP–Golgi (b, yellow channel) transfected Hela cells were loaded with CaTM-2 AM (c, red channel). d) Triple-color merged image. Scale bar: 20 μm.

Next, we examined whether CaTM-2 can detect changes in intracellular cytoplasmic Ca^{2+} concentration. HeLa cells were loaded with CaTM-2 AM and then stimulated with histamine to induce Ca^{2+} oscillation (Figure 5a–d).[24] As expected, CaTM-2 diffused uniformly throughout the cytosol, and enabled the successful visualization of changes in the cytoplasmic Ca^{2+} concentration (Figure 5d; see Supporting movie 1). Ca^{2+} spikes did not occur in all cells, and the oscillation behavior depended on the cell. We also performed the equivalent experiment with Rhod-2 AM (Figure 5e–h). In the histamine-stimulated cells, most of the areas that showed an increase in fluorescence were mitochondria (Figure 5g), in agreement with previous reports.[24–27] Thus, Rhod-2 AM mainly monitored the Ca^{2+} concentration in mitochondria, which exhibit a slower kinetic Ca^{2+} transient relative to that in the cytosol (Figure 5h; see also Supporting movie 2).[25] We examined the localization of these probes in other cell lines (COS7, A549, CHO-k1, and HEK293) and observed no distinctive compartmentalization of CaTM-2 AM inside these cells (see Figure S6 in the Supporting Information). On the other hand, Rhod-2 AM was mostly localized in compartments that appeared to be mitochondria, in accordance with previous reports (see Figures S6–S8 in the Supporting Information).[24–27]

We also compared the usefulness of CaTM-2 AM and Fura Red as fluorescence imaging agents. CaTM-2 AM could clearly detect ATP-induced Ca^{2+} oscillation and ionomycin-induced Ca^{2+} influx in HeLa cells (see Figure S9 in the Supporting Information; ATP = adenosine triphosphate). Fura Red could also be used to monitor these events, but high-power laser excitation was needed to obtain a sufficient fluorescence signal, probably because of the very low fluorescence quantum efficiency of Fura Red, and the fluorescence signal was still a little noisy (see Figure S10 in the Supporting Information). Furthermore, CaTM-2 is expected to be superior to Fura Red for Ca^{2+} imaging in biosamples, such as tissues, because the excitation and emission wavelengths of CaTM-2 both lie in the tissue-penetrating long-wavelength region, whereas Fura Red has a much shorter excitation wavelength.[28] However, Fura Red has the strong point that it can be used for ratiometric imaging, unlike CaTM-2. We utilized a commercially available dye-dispersing agent, Pluronic F-127, to assist in loading the fluorescent probe into live cells (see Figures S9 and S10).

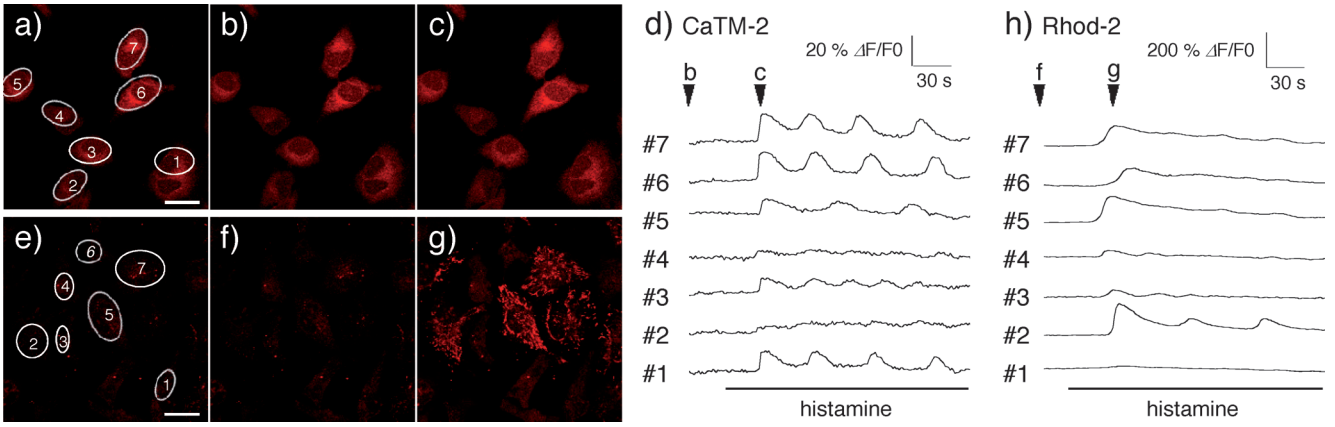

Figure 5. Visualization of histamine-induced calcium oscillations in HeLa cells with CaTM-2 AM and Rhod-2 AM. HeLa cells loaded with CaTM-2 AM (3 μM; a–d) or Rhod-2 AM (3 μM; e–h) were stimulated with histamine (1 μM). a–c) Fluorescence images of CaTM-2. Images (b) and (c) were taken at the time points indicated with arrowheads in (d). e–g) Fluorescence images of Rhod-2. Images (f) and (g) were taken at the time points indicated with arrowheads in (h). d,h) Fluorescence changes in regions of interest of individual cells numbered 1–7 in (a) and (e) are shown in (d) and (h), respectively. Scale bars: 30 μm. See also Supporting movies 1 and 2.

The use of the dispersant greatly enhanced the emission signal. Thus, the loading of CaTM-2 AM with a dispersing agent is effective in producing a large fluorescence signal, although it may have some influence on cellular homeostasis.

For the broader biological application of Ca^{2+} indicators for multicolor imaging and in vivo imaging, some red to near-infrared fluorescent probes for Ca^{2+}, CaSiR-1,[29] KFCA,[30] and Calcium Rubies[31] were recently developed. CaSiR-1 and its AM ester form are especially useful for neuronal Ca^{2+} imaging, but because of its localization in lysosomes in some types of cultured cells, CaSiR-1 AM will sometimes be unsuitable for the detailed analysis of signaling pathways inside cells (see Figures S11–S15 in the Supporting Information). Two other probes were also used successfully to monitor cytoplasmic Ca^{2+}; however, the AM ester forms of these probes were not synthesized. They were introduced into cells by bead loading[30] or through unique uptake into astrocytes.[31] Unlike these probes, CaTM-2 could be used to monitor cytoplasmic Ca^{2+} in cultured cells by using the AM ester loading method.

The fluorescence imaging of Ca^{2+} has also been used in neuroscience for the analysis of neuronal networks on the basis of increases in somatic Ca^{2+} following neuronal action potentials.[32–35] Therefore, as a further demonstration of the usefulness of CaTM-2 AM, we confirmed that it could be used to monitor the activity of neurons in cultures of rat hippocampal slices (see Supporting movie 3 and Figures S16 and S17 in the Supporting Information).

In conclusion, we have designed and developed a red fluorescent probe for cytoplasmic Ca^{2+} and confirmed its usefulness in several biological applications in cultured live cells. Because changes in the cytoplasmic concentration of Ca^{2+} are deeply related to various physiological phenomena, the ability to simultaneously monitor cytoplasmic Ca^{2+} and other metal ions or proteins is important for the detailed investigation of biological signaling pathways. The new probe can be employed in combination with various fluorophores that emit in the UV to yellow range; for example, it would be applicable in GFP-expressing animals and cultured cells. We believe that our probe will open up new possibilities for innovative approaches to address a variety of Ca^{2+}-related research problems.

Received: December 25, 2012
Revised: January 26, 2013
Published online: February 25, 2013

Keywords: bioimaging · calcium · cell signaling · fluorescence · imaging agents

[1] A. P. de Silva, H. Q. N. Gunaratne, T. Gunnlaugsson, A. J. M. Huxley, C. P. McCoy, J. T. Rademacher, T. E. Rice, *Chem. Rev.* **1997**, *97*, 1515 – 1566.
[2] G. Zlokarnik, P. A. Negulescu, T. E. Knapp, L. Mere, N. Burres, L. Feng, M. Whitney, K. Roemer, R. Y. Tsien, *Science* **1998**, *279*, 84 – 88.
[3] T. Nagano, T. Yoshimura, *Chem. Rev.* **2002**, *102*, 1235 – 1269.
[4] T. Terai, T. Nagano, *Curr. Opin. Chem. Biol.* **2008**, *12*, 515 – 521.
[5] G. Grynkiewicz, M. Poenie, R. Y. Tsien, *J. Biol. Chem.* **1985**, *260*, 3440 – 3450.
[6] A. T. Harootunian, J. P. Y. Kao, S. Paranjape, R. Y. Tsien, *Science* **1991**, *251*, 75 – 78.
[7] J. Chambers, R. S. Ames, D. Bergsma, A. Muir, L. R. Fitzgerald, G. Hervieu, G. M. Dytko, J. J. Foley, J. Martin, W.-S. Liu, J. Park, C. Ellis, S. Ganguly, S. Konchar, J. Cluderay, R. Leslie, S. Wilson, H. M. Sarau, *Nature* **1999**, *400*, 261 – 265.
[8] I. Micu, A. Ridsdale, L. Zhang, J. Woulfe, J. McClintock, C. A. Brantner, S. B. Andrews, P. K. Stys, *Nat. Med.* **2007**, *13*, 874 – 879.
[9] D. Skokos, G. Shakhar, R. Varma, J. C. Waite, T. O. Cameron, R. L. Lindquist, T. Schwickert, M. C. Nussenzweig, M. L. Dustin, *Nat. Immunol.* **2007**, *8*, 835 – 844.
[10] K. V. Kuchibhotla, C. R. Lattarulo, B. T. Hyman, B. J. Bacskai, *Science* **2009**, *323*, 1211 – 1215.
[11] M. J. Berridge, M. D. Bootman, H. L. Roderick, *Nat. Rev. Mol. Cell Biol.* **2003**, *4*, 517 – 529.
[12] D. E. Clapham, *Cell* **2007**, *131*, 1047 – 1058.
[13] A. Miyawaki, J. Llopis, R. Heim, J. M. McCaffery, J. A. Adams, M. Ikura, R. Y. Tsien, *Nature* **1997**, *388*, 882 – 887.
[14] Y. Zhao, S. Araki, J. Wu, T. Teramoto, Y.-F. Chang, M. Nakano, A. S. Abdelfattah, M. Fujiwara, T. Ishihara, T. Nagai, R. E. Campbell, *Science* **2011**, *333*, 1888 – 1891.
[15] A. Minta, J. P. Y. Kao, R. Y. Tsien, *J. Biol. Chem.* **1989**, *264*, 8171 – 8178.
[16] "Monitoring Cell Calcium": R. Y. Tsien in *Calcium as a Cellular Regulator* (Eds.: E. Carafoli, C. Klee), Oxford University Press, New York, **1999**, pp. 28 – 54.
[17] *The Molecular Probes® Handbook: A Guide to Fluorescent Probes and Labeling Technologies*, 11th ed. (Eds.: I. Johnson, M. T. Z. Spence), Molecular Probes, Eugene, OR, **2010**.
[18] S. M. Ward, T. Ördög, S. D. Koh, S. A. Baker, J. Y. Jun, G. Amberg, K. Monaghan, K. M. Sanders, *J. Physiol.* **2000**, *525*, 355 – 361.
[19] J. P. Y. Kao, G. Li, D. A. Auston, *Methods Cell Biol.* **2010**, *99*, 113 – 152.
[20] T. Egawa, Y. Koide, K. Hanaoka, T. Komatsu, T. Terai, T. Nagano, *Chem. Commun.* **2011**, *47*, 4162 – 4164.
[21] Y. Urano, M. Kamiya, K. Kanda, T. Ueno, K. Hirose, T. Nagano, *J. Am. Chem. Soc.* **2005**, *127*, 4888 – 4894.
[22] W. Göbel, F. Helmchen, *Physiology* **2007**, *22*, 358 – 365.
[23] K. Takemoto, T. Nagai, A. Miyawaki, M. Miura, *J. Cell Biol.* **2003**, *160*, 235 – 243.
[24] D.-M. Zhu, E. Tekle, C. Y. Huang, P. B. Chock, *J. Biol. Chem.* **2000**, *275*, 6063 – 6066.
[25] G. Hajnóczky, L. D. Robb-Gaspers, M. B. Seitz, A. P. Thomas, *Cell* **1995**, *82*, 415 – 424.
[26] T. J. Collins, P. Lipp, M. J. Berridge, M. D. Bootman, *J. Biol. Chem.* **2001**, *276*, 26411 – 26420.
[27] M.-J. Jou, T.-I. Peng, S.-S. Sheu, *J. Phys.* **1996**, *497*, 299 – 308.
[28] R. Weissleder, *Nat. Biotechnol.* **2001**, *19*, 316 – 317.
[29] T. Egawa, K. Hanaoka, Y. Koide, S. Ujita, N. Takahashi, Y. Ikegaya, N. Matsuki, T. Terai, T. Ueno, T. Komatsu, T. Nagano, *J. Am. Chem. Soc.* **2011**, *133*, 14157 – 14159.
[30] A. Matsui, K. Umezawa, Y. Shindo, T. Fujii, D. Citterio, K. Oka, K. Suzuki, *Chem. Commun.* **2011**, *47*, 10407 – 10409.
[31] M. Collot, C. Loukou, A. V. Yakovlev, C. D. Wilms, D. Li, A. Evrard, A. Zamaleeva, L. Bourdieu, J.-F. Léger, N. Ropert, J. Eilers, M. Oheim, A. Feltz, J.-M. Mallet, *J. Am. Chem. Soc.* **2012**, *134*, 14923 – 14931.
[32] R. Cossart, D. Aronov, R. Yuste, *Nature* **2003**, *423*, 283 – 288.
[33] Y. Ikegaya, G. Aaron, R. Cossart, D. Aronov, I. Lampl, D. Ferster, R. Yuste, *Science* **2004**, *304*, 559 – 564.
[34] Z. F. Mainen, R. Malinow, K. Svoboda, *Nature* **1999**, *399*, 151 – 155.
[35] Y. Kovalchuk, J. Eilers, J. Lisman, A. Konnerth, *J. Neurosci.* **2000**, *20*, 1791 – 1799.

